Quantum-mechanical phase interference and optical polarization in low-energy Na^+-Ne inelastic collisions

N. H. Tolk, J. C. Tully, C. W. White, J. Kraus, A. A. Monge, D. L. Simms, and M. F. Robbins
Bell Laboratories, Murray Hill, New Jersey 07974

S. H. Neff
Earlham College, Richmond, Indiana 47347

W. Lichten*
Yale University, New Haven, Connecticut 06520

(Received 13 November 1975)

Pronounced oscillatory structure and strong optical polarization effects have been observed in emission cross sections for the production of optical radiation measured as a function of energy in low-energy (100 eV to 6 keV) Na^+-Ne atomic collisions. Highly regular oscillatory structure found in the energy dependence of the emission cross sections for ten NeI($3p \rightarrow 3s$) optical transitions is observed to be in antiphase with similar structure in two NaI($3p \rightarrow 3s$)optical emission cross sections. In addition, large polarization effects have been observed in optical radiation from excited $J \neq 0$ states. In one particular case involving a $J = 1$ to $J = 0$ transition, oscillations in the excitation function appear to arise exclusively from the polarization component of the radiation perpendicular to the beam direction. These observations indicate strong sublevel-state selection processes associated with collisional quantum-mechanical phase-interference phenomena. A simple model is presented which allows us to uniquely determine for the first time the quasimolecular states responsible for such oscillatory structure and consequently associated with each polarization component. Analysis based on the model for the case of the Na*($3p$) radiation data indicates that the oscillatory structure is not attributable to interactions between simple single-electron diabatic states as believed previously. Similar analysis of the Ne*($3p$) radiation data uniquely identifies the $^1\Pi(\Omega = \pm 1)$ and $^3\Pi(\Omega = \pm 2)$ molecular states as the major contributors.

I. INTRODUCTION

Our understanding of the quasimolecular processes leading to outer-shell excitation in ion-atom heavy-particle collisions has progressed rapidly over the past ten years.[1] Recent experimental data on total emission cross sections have provided an unexpectedly varied and complex array of interesting results.[2,3] These results are sensitive to the detailed nature of the molecular potentials and their interactions. In this work, we have made a study of collisional excitation in low-energy (100 eV to 6 keV) Na^+-Ne collisions and have measured absolute emission cross sections for each polarization component as a function of bombarding energy for optical transitions arising from excited $3p$ electrons in NeI and NaI. Our measurements show highly regular oscillations in the Na^+-Ne cross sections obtained as a function of energy. The emission cross sections measured for the ten levels arising from transitions from the $3p$ levels of NeI exhibit oscillatory structure of the same spacing and phase. The NaI cross sections also show oscillations alike in spacing and phase, but in antiphase with the NeI($3p$) cross sections.

In many instances, we observe strong polarization effects in the optical radiation arising from collisional excitation of NeI($3p$) states. In one case where radiation originates from a $J = 1$ to $J = 0$ transition in NeI, oscillatory structure in the energy dependence of the emission cross section is measured to be due entirely to the component of the emitted radiation polarized perpendicularly to the incident-beam direction. This is the first experimental measurement of regular quantum-mechanical phase-oscillatory structure arising from a single optical polarization component and therefore from a single set of magnetic sublevels. These measurements consequently allow us for the first time to develop a simple model which relates the final atomic excited states to the quasimolecular states which participate in the quantum-mechanical phase-interference process. We have identified the $^1\Pi(\Omega = \pm 1)$ and $^3\Pi(\Omega = \pm 2)$ states as the major contributors to the quantum-mechanical phase-interference processes, and not the simple single-electron diabatic states as believed previously.[2,3] Using this model, we have been able to account quantitatively for the magnitudes of the oscillation amplitudes in the polarization components of the NeI and NaI emission cross sections.

II. APPARATUS

The Na^+-Ne results were obtained using a low-energy ion accelerator capable of producing ion beams of well-defined energy ($\Delta E < 1$ eV) in the range from 10 eV to 6 keV with beam particle currents varying from 10^{12} particles/sec at 10 eV to 10^{14} particles/sec at 6.0 keV. The beam was directed using electrostatic lenses from the source chamber through an intermediate pumping region into the collision chamber. Optical radiation from the collision region was measured at 90° with respect to the beam direction using a 0.3-m $f/5$ monochromator and an S-20Q phototube. Sensitive single-photon counting techniques were used to detect and process the photon signals. An EOA L-101 Spectral Irradiance Standard employing a calibrated tungsten coiled-coil quartz-iodine lamp was used to determine the absolute spectral response of the system. Polarization data were acquired with a Polaroid HN-38 polarizer. Gas pressure information was obtained using a calibrated capacitance manometer. Photon counting rates, particle current data, and pressure measurements were processed using an on-line PDP-8 computer to calculate absolute emission cross sections.

The sensitivity of the optical collection system and photon counting apparatus was determined for both senses of polarization at the wavelengths corresponding to each of the emission lines of interest by using the standard lamp for calibration. We estimate the uncertainty in the absolute sensitivity determined in this manner to be ±50%. This therefore is a lower limit to the uncertainty in the absolute magnitude of the individual cross sections. Comparison of cross sections of the same optical line at the two senses of polarization should be significantly better; we estimate this uncertainty to be $\leq \pm 5\%$.

The Ne* and Na* emission cross sections as a function of energy were measured in the single-collision regime as determined by linearity in the measurements of photon signal versus pressure. No corrections have been applied to our data owing to effects associated with cascading transitions, but these effects are estimated to be less than 10%. In all cases, we find the structure in the individual emission cross sections to be reproducible from run to run to better than 5% with respect to both amplitude and energy.

III. RESULTS

Most of the visible Ne I radiation within the wavelength region studied (2000–8000 Å) arises from ten levels which are in the $2p^5(^2P^o_{3/2})3p$ and $2p^5(^2P^o_{1/2})3p$ configurations as shown in Fig. 1. In addition, most of the sodium radiation originates from the two Na $D(3p)$ levels also shown in Fig. 1. Thus radiation observed in the Na^+-Ne experiment arises from the excitation of both Ne and Na into $3p$ electronic states as a result of direct and charge-exchange collision processes,

$$Na^+ + Ne \rightarrow \begin{cases} Na^+ + Ne^*(3p) \\ Na^*(3p) + Ne^+ \end{cases} .$$

Figures 2(a) and 2(b) show 12 sets of absolute emission cross sections plotted as a function of ion-beam energy for the perpendicular and parallel polarization components of Ne I$(3p \rightarrow 2s)$ and Na $D(3p \rightarrow 2s)$ radiation arising from Na^+-Ne collisions. In each case, the data were taken under single-collision conditions in the linear region of the photon-signal–versus–pressure curve. Except for the two $J = 0$ cases, $2p_1$ and $2p_3$ (Paschen notation), the emission cross sections measured for the populations of the Ne I$(3p)$ levels all show regular oscillatory structure of the same spacing and phase. The two Na D emission cross sections also show oscillations alike in spacing and phase,

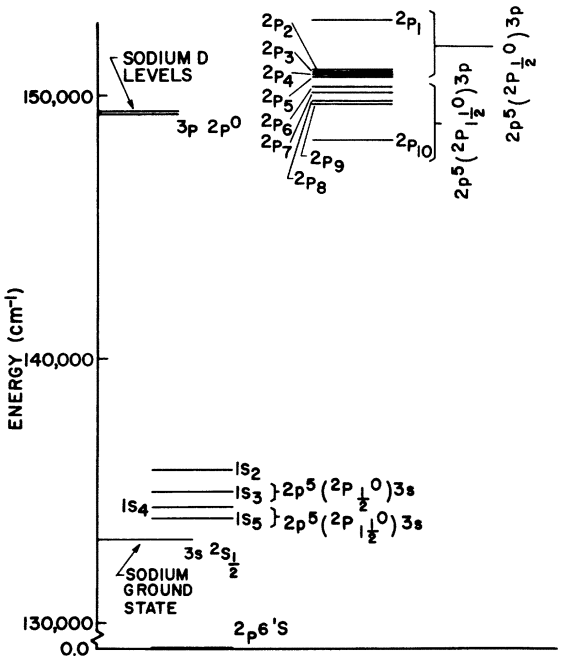

FIG. 1. Schematic illustration of the minimum energy required to populate Ne$(3s)$ and Ne$(3p)$ levels by direct excitation and Na D_1 and Na D_2 levels by charge exchange excitation owing to Na^+-Ne collisions. The sodium and neon energy levels shown represent the location of the energy levels of the $(NaNe)^+$ system at infinite internuclear distance.

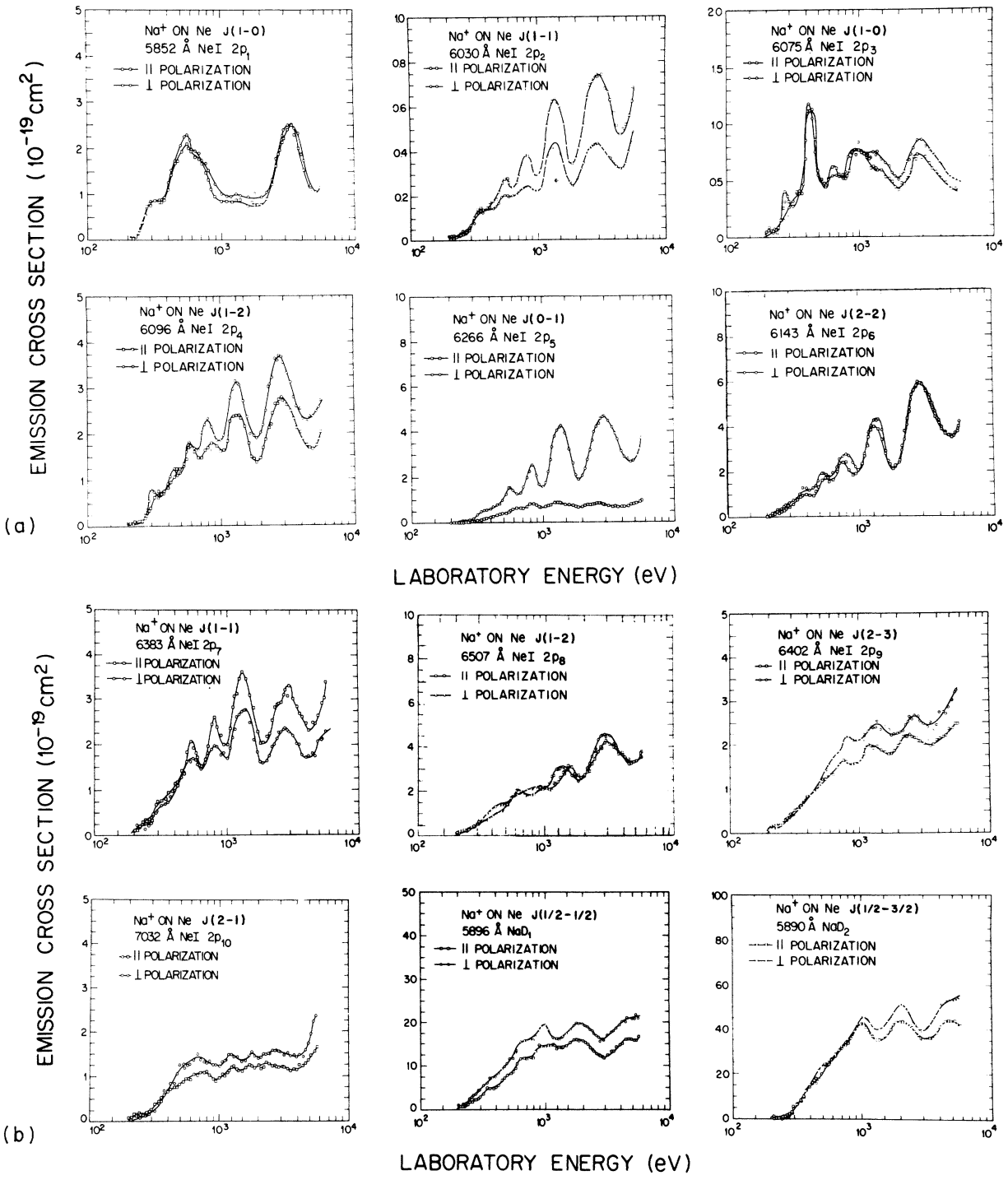

FIG. 2. Absolute emission cross sections, plotted as a function of bombarding energy, for the perpendicular and parallel components of optical radiation emitted at 90° from the beam direction. (a) The radiation comes from optical transitions arising from the decay of $3p$ electrons in Ne I excited by Na^+-on-Ne collisions. Results are shown for six of the ten levels in the $2p^5(3p)$ configurations in Ne I. (b) The radiation comes from optical transitions arising from the decay of $3p$ electrons in Ne I and Na I excited by Na^+-on-Ne collisions. Results are shown for four of the ten levels in the $2p^5(3p)$ configurations in Ne I and from the two Na D levels. The structure in the cross sections is reproducible to better than 5%, the relative magnitude between each of the two polarization components are uncertain to 5%, and the absolute magnitudes of the total emission cross sections are uncertain to 50%.

but in antiphase with the Ne I structure observed.

Polarization fraction data plotted as a function of laboratory ion-beam energy is shown in Fig. 3 along with the perpendicular and parallel components of the absolute emission cross sections for the excitation of the 6266-Å Ne I optical emission line owing to Na^+-Ne collisions. The polarization fraction Π is defined in the usual manner:

$$\Pi = (I_{\parallel} - I_{\perp})/(I_{\parallel} + I_{\perp}) , \quad (1)$$

where $I_{\parallel}$ and $I_{\perp}$ are photon intensities measured with polarizer parallel and perpendicular to the beam direction. Polarization anisotropy has been accounted for in Fig. 3 but not in Fig. 2. Figure 3 represents a particularly favorable case in-

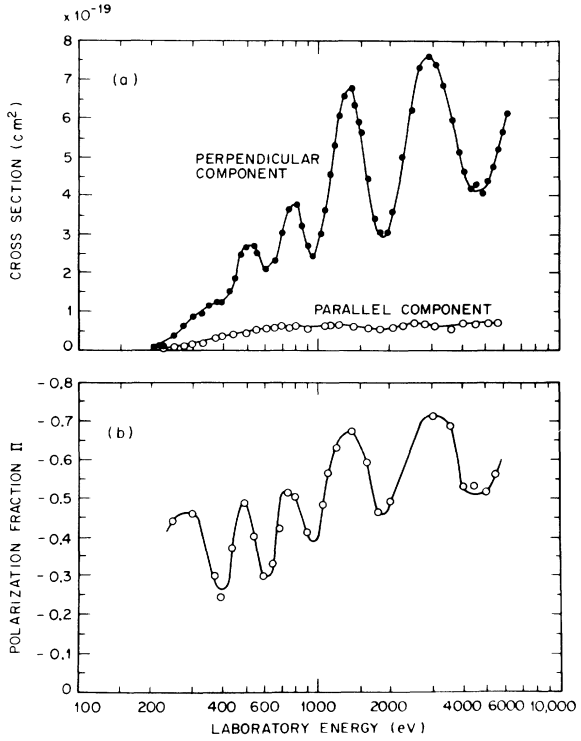

FIG. 3(a). Absolute emission cross sections as a function of ion-beam energy for the perpendicular and parallel components of Ne I 6266-Å radiation arising from low-energy Na^+-Ne collisions. These components have been corrected for intensity anisotropy such that the sum will give the total absolute emission cross sections. The structure in the cross sections is reproducible to better than 5%, while the absolute magnitudes of the total emission cross sections are uncertain to 30%. The small amount of structure present in the parallel component may be attributed to an imperfect polarizer, a finite acceptance angle, and the inexactness of hypothesis (d). (b) Polarization fraction $\Pi = (I_{\parallel} - I_{\perp})/(I_{\parallel} + I_{\perp})$ as a function of ion-beam energy for Ne I 6266-Å radiation (arising from a $J=1$ to $J=0$ transition) as a result of Na^+ +Ne collisions.

volving a $J=1$ to $J=0$ transition. It should be noted in this case that the absolute value of the polarization fraction is surprisingly large and that the appearance of the data is consistent with the assumption that all of the oscillatory structure arises from the polarization component perpendicular to the ion-beam direction.

Assuming effects due to cascading transitions are negligible, absolute cross sections for populating the ten Ne($3p$) and two Na($3p$) fine-structure states can be obtained from the measured absolute emission cross sections. Since many of the Ne I $3p$ levels can radiate to more than one lower state, this requires taking proper account of branching ratios. Total cross sections for formation of each level can be written in the form

$$\sigma_{\text{total}} = \tfrac{2}{3}\sigma_{\parallel} + \tfrac{4}{3}\sigma_{\perp} , \quad (2)$$

where

$$\sigma_{\parallel} = \sigma_{\parallel}^{(\text{rad})} B_i , \quad (3)$$

$$\sigma_{\perp} = \sigma_{\perp}^{(\text{rad})} B_i . \quad (4)$$

$\sigma_{\parallel}^{(\text{rad})}$ and $\sigma_{\perp}^{(\text{rad})}$ are the measured absolute emission cross sections for parallel and perpendicular polarization, respectively. B_i is the inverse of the branching ratio for the appropriate transition i,

$$B_i = \sum_j \frac{A_j}{A_i} , \quad (5)$$

where A_j is the radiative transition probability to lower state j. Branching ratios were obtained from transition probabilities reported by Bennett and Kindlman[4] and by Schectman *et al.*,[5] and are listed in Table I. The total cross section for

TABLE I. Inverse ratios $\sum_j A_j/A_i$, where A_i are transition probabilities derived from the work of Bennett and Kindlmann (Ref. 4) and of Schectman *et al.* (Ref. 5).

State	Line (Å)	No. of allowed transitions	$\sum_j A_j/A_i$
$2p_1$	5852	2	1.01
$2p_2$	6030	4	11.08
$2p_3$	6075	2	1.02
$2p_4$	6096	3	3.35
$2p_5$	6266	4	2.22
$2p_6$	6143	3	2.20
$2p_7$	6383	4	1.66
$2p_8$	6507	3	1.75
$2p_9$	6402	1	1.00
$2p_{10}$	7032	4	1.66

formation of Ne($3p$), obtained by summing σ_{total} over all ten Ne($3p$) levels, is shown in Fig. 4. The total cross section for formation of Na($3p$), obtained by summing over the two Na D levels, is also shown in Fig. 4. Note that (i) the oscillations in the two cross sections are 180° out of phase,[6-8] (ii) the amplitudes of the oscillations in the two cases are approximately equal, and (iii) the magnitudes of the average cross sections for production of Na*($3p$) and Ne*($3p$) are in the ratio of approximately 3:2 at the intermediate and higher energies.

Observations (i) and (ii) support the hypothesis that oscillatory structure is due to interference between quasimolecular states of the $(NeNa)^+$ collision system associated with direct and charge exchange processes. This is consistent with the energy levels of $(NaNe)^+$ at infinite internuclear separation. As shown in Fig. 1, the Na D levels fall within the energy range over which the Ne($3p$) levels are distributed and are consequently nearly degenerate. Both sets of cross sections are measured to have the same energy thresholds within experimental error at approximately 120 eV in the center-of-mass sytem which is about 100 eV above that required for populating the levels calculated strictly on the basis of conservation of energy. This is further evidence that the participating levels are coherently populated.[9]

Figure 5 shows the total cross section for the population of the $3p$ levels [ten Ne*($3p$) and two Na*($3p$) levels] plotted as a function of laboratory energy owing to Na^+-on-Ne collisions derived by summing the two cross sections shown in Fig. 4. Although the markedly regular oscillations have disappeared, there persists some structure, notably a depression at about 1800-eV laboratory energy. This structure may be attributed either to cascade effects or to intrinsic characteristics of the cross section itself. The relative smoothness of the curve is further evidence that we have identified correctly the interfering channels as associated with charge exchange and direct excitation channels.

IV. ANALYSIS OF RESULTS

Several authors have pointed out how the presence of at least two states in interference can lead to multiple frequencies of oscillation of light intensity, plotted as a function of inverse velocity in the exit channels.[1] In the present case, there are more than enough molecular states to explain any variation in the frequency of oscillatory structure among any of the twelve lines and their polarization components. The problem is to explain the relative simplicity of our results. Why does only a single oscillatory pattern appear? Why do the neon levels tend to oscillate in phase with each other and the sodium levels oscillate in antiphase? Why are such strong polarization effects observed? And why does the amplitude of the oscillatory structure vary so widely from one neon level to another?

In order to shed light on these questions, we invoke the following four hypotheses[10]:

(a) Oscillations in the energy dependence of the

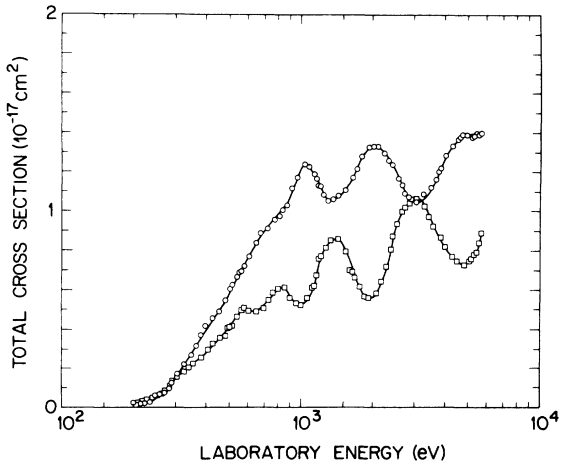

FIG. 4. Absolute population cross sections for the Ne*($3p$) levels (–□–□–) and Na*($3p$) levels (–○–○–) plotted as a function of laboratory energy.

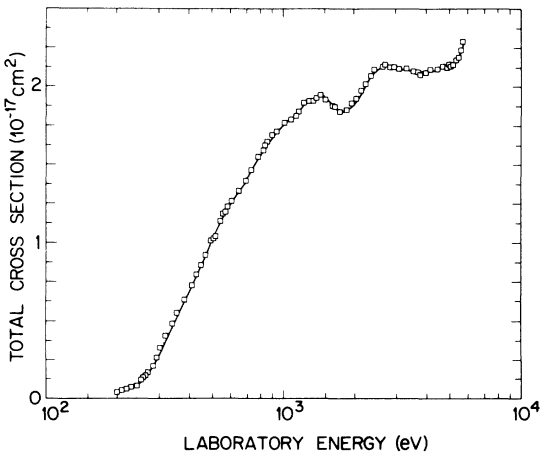

FIG. 5. Absolute cross section for populating the $3p$ electron in the $(NaNe)^+$ system plotted as a function of laboratory energy. This is the sum of the two cross sections shown in Fig. 4.

cross sections result from interference between one or more pairs of excited levels which are populated coherently at small internuclear separation and then interact at large separation, as illustrated schematically in Fig. 6. This dual-coupling mechanism, first proposed by Rosenthal and Foley,[11] has been established in several related atomic collision processes.[1]

(b) Nonadiabatic interaction at large internuclear separation arises from "quasiresonant charge exchange" of the type described by Lichten.[12]

(c) The distribution of final atomic level populations, through the quantum-mechanical sudden approximation, is a direct reflection of the composition of the precursor molecular electronic states. This hypothesis is stated below in mathematical terms, and it allows us to account quantitatively for the cross sections for formation of various excited Na and Ne levels.

(d) At the outer coupling region, the molecular axis coincides with the laboratory z direction. This hypothesis, approximately valid for low-angle scattering, greatly simplifies the analysis of polarization data.

We discuss each of these hypotheses in detail below, and then examine their consequences.

A. Dual-coupling model [hypothesis (a)]

The Rosenthal-Foley model[11] can be broken down into three separate parts:

(i) The primary excitation mechanism, in which a transition is made from the ground U_0 state to at least two inelastic channels U_1 and U_2 (at the inner internuclear separation R_i in Fig. 6).

(ii) The inelastic channels U_1 and U_2, between which a phase difference develops during the outgoing part of the collision ($R_i \leq R \leq R_0$ in Fig. 6).

(iii) A second interaction region (at the outer internuclear separation R_0 in Fig. 6), at which interference occurs between the inelastic channels.

It can be easily shown[2] that the phase difference $\Delta\varphi$ developed in the interval R_i to R_0 during the outgoing part of the collision can be expressed approximately as

$$\Delta\varphi = (1/\hbar)\langle ER\rangle/v + \Delta\varphi_0, \tag{6}$$

where $\langle ER\rangle$ is the area between curves bounded by the two interaction regions at R_i and R_0,

$$v^2 = (2/m)(E - U) \simeq (2/m)(E - U_{av}) , \tag{7}$$

and $\Delta\varphi$ is the initial phase difference which would result from an infinitely fast collision. It can also be easily shown that the cross section is proportional to $\cos^2(\frac{1}{2}\Delta\varphi)$. Consequently it will exhibit maxima (minima) whenever the following condition is met:

$$\Delta\varphi = 2\pi n = (1/\hbar)\langle ER\rangle/v + \Delta\varphi_0 . \tag{8}$$

The above expression suggests that if cross-section data are plotted as a function of $1/v$, assuming a proper choice of U_{av}, then the maxima should be equally spaced. An integer n may be assigned to each maximum such that, for example, $n=1$ refers to the first peak which appears as v decreases from infinite velocity. The y intercept of a plot of n vs $1/v$ will give the initial phase difference to an additive integral multiple of 2π, and the quantity $\langle ER\rangle$, which is important for comparison with calculated potential curves, can be derived from the slope of the line.

In Fig. 7, this analysis is applied to the Ne I 6266-Å emission cross section due to Na^+-Ne collisions. The upper portion shows the 6266-Å cross section plotted as a function of $1/v$. The lower portion of Fig. 7 is a line plot which when extrapolated to infinite velocity gives an integer initial phase. It is important to consider the proper criteria for choosing the correct U_{av} to be used in calculating the quantity v. Two criteria are possible: The first is that U_{av} be chosen to lie between the minimum excitation energy allowed by conservation of energy and the actual energy threshold and that its specific value be that which occurs when the distances between maxima in the cross section be most equally spaced when plotted versus $1/v$; the second criterion is that the initial phase difference should be a simple expression (for example, either an integral or a half-integral

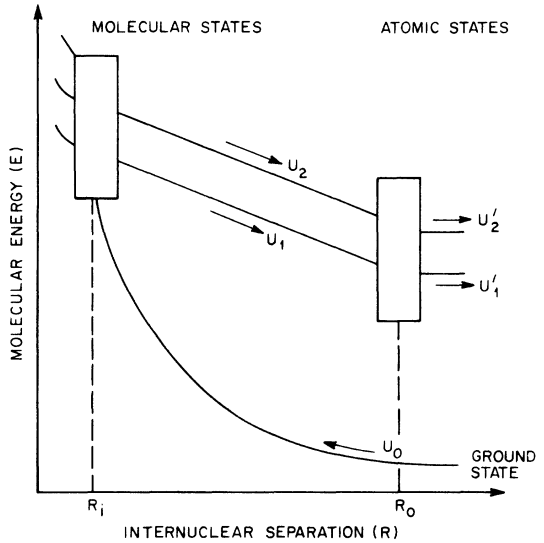

FIG. 6. Schematic illustration of the dual-interaction model.

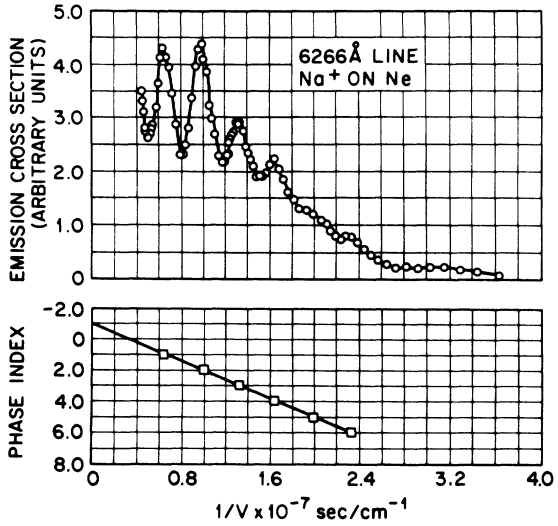

FIG. 7. Absolute emission cross section for the 6266-Å line owing to $Na^+ + Ne$ collisions plotted as a function of $1/v$, $[(2/m)(E-U)]^{1/2}$, with E the center-of-mass energy and U the average excited-state energy above the ground state. For this plot $U = 60$ eV. The straight line at the bottom portion of the figure is a linear least-squares fit of the phase integers n vs the locations in $1/v$ of maxima in the cross section.

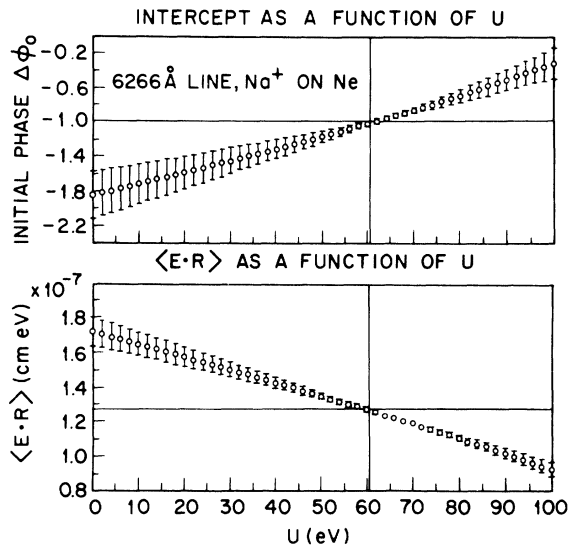

FIG. 8. Index n of the initial phase difference $\Delta\varphi_0$ (the phase difference at infinite velocity) and $\langle ER\rangle$ plotted as a function of U, the average excited-state energy above the ground state. The error bars are variances which indicate the degree to which the distances between the maxima in the cross section are equal.

multiple of 2π). In Fig. 8 the initial phase difference $\Delta\varphi_0$ (in units of n) and the quantity $\langle ER\rangle$ are plotted as a function of U_{av}. The error bars associated with each point are variances whose magnitudes reflect the degree to which the distances between the maxima are equal. The peaks are seen to be most equally spaced when U_{av} equals approximately 60 eV (the value used in the plot in Fig. 7) and $\langle ER\rangle$ equals about 1.27×10^{-7} eV cm. This also occurs when $\Delta\varphi_0$ is an integral multiple of 2π and consequently both of the above criteria are satisfied. This is similar to values of $\langle ER\rangle$ found in the $(HeNe)^+$ collision case.[1] In Fig. 9, the same analysis is applied to the Na D_2 5890-Å cross section, again using the value $U_{av} = 60$ eV to calculate v. Similar results are found with the not surprising exception that the initial phase is a half-integral multiple of 2π.

The above analysis provides a quantitative measure of the average energy and splitting between the interacting excited states responsible for the observed oscillatory behavior, but it does not identify these states. To do this we first need to examine the electronic character of the $(NaNe)^+$ molecular states.

The colliding atoms approach initially along the $^1\Sigma^+$ ground-state potential curve of $(NeNa)^+$. This curve is very repulsive, reflecting the behavior of two rare-gas-like atoms; thus at small inter-

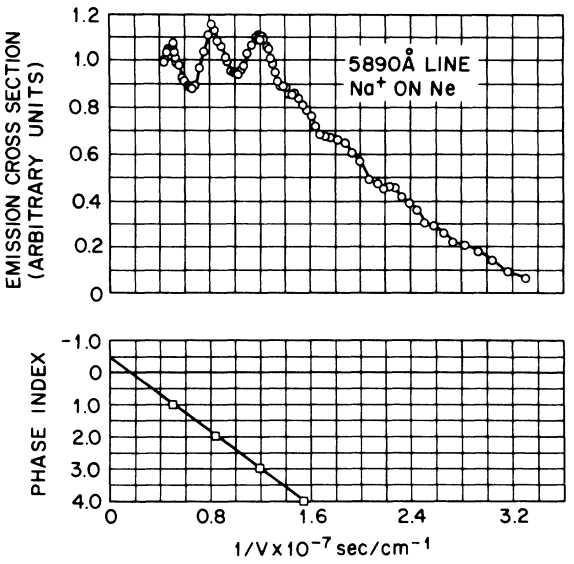

FIG. 9. Absolute emission cross section for the 5890-Å Na D_2 line owing to $Na^+ + Ne$ collisions plotted as a function of $1/v$. For this plot $U = 60$ eV. The straight line at the bottom portion of the figure is a linear least-squares fit of the phase integers n vs the locations in $1/v$ of the maxima in the cross sections.

nuclear separations it will interact strongly with excited-state curves. We are interested particularly in those excited states which at large internuclear separation correlate with $Ne^*(2p^5, 3p) + Na^+$ and $Na^*(3p) + Ne^+(2p^5)$. At moderate-to-large internuclear separation, these excited states can be accurately described as one-electron states outside of a $Na^+(2p^6)$-$Ne^+(2p^5)$ core. Configurations corresponding to excitation of the Na^+ core or inner-shell excitation of Ne would be associated with too high an energy to contribute significantly in this region.[13]

The symmetry of the $Na^+(2p^6)$-$Ne^+(2p^5)$ core must be either $^2\Sigma^+$ or $^2\Pi$, since it is produced by removal of one electron from $Ne(^1S)$; i.e., the vacant $2p$ orbital may have σ or π symmetry. Similarly, the outer $3p$ electron can occupy molecular orbitals of either σ or π symmetry. The $(NaNe)^+$ molecular states can be derived by combining a core state and outer-electron state according to the rules given by Herzberg, as shown in Table II.[14] The subscripts on the molecular states indicate the value of $\Omega = \Lambda + \Sigma$ (Ω is the sum of the orbital Λ and spin Σ projections along the internuclear axis). There are two of each of the states listed (Na^+-Ne and Na-Ne^+), resulting in 72 states in all.

A very rough estimate of the relative energies of the molecular states suggests that the energy splitting between the two possible Na^+Ne^+ core states is comparable with that between the various outer-electron states.[15] Therefore we would expect that at least some of the molecular states might be composed of mixtures of one-electron configurations of the same symmetry and similar energy; i.e., a molecular state might not be dominated by a single diabatic configuration. In addition, at large internuclear separations spin-orbit interaction becomes comparable to the splitting between states; thus states with the same value of $\Omega = \Sigma + \Lambda$ may mix strongly in this region. As discussed below, the importance of both of these effects is established conclusively by our experimental results. Primary excitation must occur at small internuclear separations where the energies of the repulsive $NaNe^+$ ground state and the excited states are similar. The excitation is viewed as a one-electron process; i.e., a $2p$ electron of Ne is promoted to one of the excited molecular orbitals listed in Table II. Both radial and rotational coupling may be important in the inner interaction region; thus the projection of orbital angular momentum along the internuclear axis need not be conserved during the excitation process. We might expect spin to remain unchanged during excitation (the Wigner spin-conservation rule). However, our results show conclusively that spin is *not* conserved; both singlet and triplet excited states are produced during the collision. This is consistent with the anticipated magnitude of spin-orbit coupling in the excited states of $(NeNa)^+$.

TABLE II. Molecular states derived from core- and outer-electron states (Ref. 14). The subscripts on the molecular states refer to values of Ω.

	Core state	Outer-electron state	Molecular states in $\Lambda\Sigma$ coupling
(a)	$^2\Sigma^+$	$^2\sigma$	$^1\Sigma^+_0$, $^3\Sigma^+_{0,\pm1}$
(b)	$^2\Pi$	$^2\sigma$	$^1\Pi_{\pm1}$, $^3\Pi_{0,0,\pm1,\pm2}$
(c)	$^2\Sigma^+$	$^2\pi$	$^1\Pi_{\pm1}$, $^3\Pi_{0,0,\pm1,\pm2}$
(d)	$^2\Pi$	$^2\pi$	$^1\Sigma^+_0$, $^3\Sigma^+_{0,\pm1}$, $^1\Sigma^-_0$, $^3\Sigma^-_{0,\pm1}$, $^1\Delta_{\pm2}$, $^3\Delta_{\pm1,\pm2,\pm3}$

B. Quasiresonant charge exchange [hypothesis (b)]

According to the Rosenberg-Foley model, states are excited coherently during primary excitation, evolve independently in the intermediate region, and are then recombined in an outer interaction region.[11] We hypothesize that in this case nonadiabatic coupling in the outer region is due to quasiresonant charge exchange. As indicated in Fig. 1, the $Na^*(3p)$-Ne^+ and Na^+-$Ne^*(3p)$ levels are nearly degenerate. In analogy to the discussion of Lichten,[12] we propose that at moderate internuclear separations (e.g., between roughly 3 and 10 Å), Na^+ and Ne^+ appear very similar to an excited $3p$ electron. Therefore the orbitals of the outer electron can be very roughly characterized as approximately *gerade* (g) or *ungerade* (u). In order of increasing energy, these orbitals may be labeled σ_g, π_u, π_g, and σ_u, with σ_g the most strongly bonding and σ_u the most strongly antibonding. Nonadiabatic transitions are associated with the changeover from the nearly g and u character of the orbitals of the outer electron at intermediate internuclear separations to the asymptotic situation where the outer electron resides either on the Ne^+ or on the Na^+. This changeover occurs at distances where the splitting between the g and u states becomes comparable to the asymptotic splitting between the $Na^*(3p)$ and $Ne^*(3p)$ states. We estimate this to be 10–15 Å.

The hypothesis that coupling in the outer interaction region is due to the quasiresonant charge exchange mechanism [hypothesis (b)] is strongly reinforced by the observations that Na* and Ne* oscillations occur 180° out of phase and the am-

plitudes of the oscillations are approximately equal (Fig. 4). Note that if the g and u symmetry were exact then the average ratio of Na*(3p)-to-Ne*(3p) populations would be unity. The experimentally measured ratio of about 1.5 (see Fig. 4) thus provides an indication of the deviation from exact resonance.

C. Population of atomic levels [hypothesis (c)]

At relatively large internuclear separations the electronic wave functions of $(NaNe)^+$ molecular states correlating with Na*(3p)-Ne^+ and Na^+-Ne*(3p) can be expressed accurately as linear combinations of atomic states:

$$\Phi_k \cong c_k \sum_{i=1}^{6} \sum_{j=1}^{6} a_{ijk}\xi_i\varphi_j^+ + (1-c_k^2)^{1/2} \sum_{i=1}^{36} b_{ik}\xi_0^+\varphi_i , \tag{9}$$

where $k = 1, \ldots, 72$; Φ_k is an adiabatic molecular wave function, and ξ_i, ξ_0^+, φ_i, and φ_j^+ are wave functions of atomic Na(3p), $Na^+(^1S)$, Ne(3p) and $Ne^+(^2P_{1/2}, {}^2P_{3/2})$, respectively. The coefficients a_{ijk} and b_{ik} are elements of a unitary transformation relating the spin and orbital angular momentum coupling scheme of the molecular states to that of the isolated atom states. The coefficients c_k describe the relative mixing of the Na^+-Ne* and Na*-Ne^+ configurations in Φ_k. The rapid variation of c_k with internuclear separation in the outer coupling region, $R \sim R_0$, is responsible for the quasiresonant charge exchange mechanism, hypothesis (b).

Hypothesis (c) can be stated in two parts: (i) The relative populations of excited atomic Ne*(3p) levels arising from a particular $(NaNe)^*$ molecular state are proportional to the intermediate internuclear separation values of $|b_{ik}|^2$ of Eq. (9); and (ii) the relative populations of excited Na*(3p) levels are proportional to $\sum_j |a_{ijk}|^2$. This hypothesis is applicable at high nuclear velocities where the quantum-mechanical sudden approximation is valid. It is difficult to ascertain *a priori* whether this high-velocity limit is attained in the present case at the collision energies studied. Hypothesis (c) requires that the projections along the internuclear axis of both spin and orbital angular momentum, Σ and Λ, be separately conserved as the atoms recede at large internuclear separation. It should be accurate to assume that the projection of total angular momentum, $\Omega = \Sigma + \Lambda$, be conserved since at large separation nonadiabatic interaction is due almost entirely to radial coupling. Angular velocities are too small to be effective. Separate conservation of Σ and Λ requires, in addition, that spin-orbit coupling be too weak to promote transitions at large internuclear separation. Whether this is true at the nuclear velocities encountered here depends upon the spacial extent of the spin-orbit recoupling region; i.e., the region where molecular interactions are about the same magnitude as the asymptotic separations of the Ne* lines (~0.1 eV). We estimate this width to be of order $2a_0$. If this estimate is correct, hypothesis (c) should be valid except perhaps at the lowest collision energies studied. Ultimately, of course, our strongest justification for invoking this hypothesis is the simplicity and accuracy of the resulting interpretation of our experiments, as discussed below.

Note that the spin-orbit recoupling region does not necessarily coincide with the outer coupling region in which quasiresonant charge exchange occurs. Angular momentum recoupling and charge transfer are independent processes. We could have made hypothesis (c) stronger by including a third part: (iii) The populations of Na* and Ne* levels are proportional to c_k^2 and $1 - c_k^2$, respectively. This would be equivalent to assuming completely diabatic motion at large internuclear separations. Although it may well be satisfied at the higher collision energies studied here, this stronger version of hypothesis (c) is not required for the interpretation given below.

As a consequence of hypothesis (c), a particular pattern of atomic level populations can serve as a "fingerprint" of the precursor molecular state. As illustrated below, populations of the Ne*(3p) levels provide information about both the Ne^+ core and the outer 3p electron; M_l and M_s of the excited neon are the sum of $\Lambda + \lambda$ and $\Sigma + \sigma$ of the Ne^+Na^+ core and the excited electron. On the other hand, Na*(3p) levels reflect solely the properties of the outer 3p electron; M_l and M_s of excited sodium will be equal to λ and σ of the outer electron. Therefore by combining experimental information about both Na* and Ne* excited states we can obtain complete information about the outer electron, the core, and the $NeNa^+$ molecular states.

D. Polarization of emitted optical radiation [hypothesis (d)]

Since the processes contributing to the oscillatory phenomena involve predominantly small-angle scattering such that the sodium-beam particles are not significantly deflected from the beam direction (the laboratory z direction), then at the outer coupling region *the molecular axis coincides with the laboratory z direction*. Therefore by hypothesis (c) the laboratory M_j value of the final atomic state, which governs the polarization of emitted light, is equal to the Ω value of the molecular state from which it was formed. Be-

cause the outer coupling region occurs at finite internuclear separation ($\gtrsim$10 Å) and the collisions occur at nonzero impact parameters, the assumption that the molecular z axis coincides with the laboratory z axis is not exact. This will result in some smearing of observed polarization.

The contributions to the polarization components of each of the 12 optical lines studied from the appropriate atomic M_j states were determined in the standard way from the transformation rules found in Condon and Shortly.[16] Examples are given for the $2p_5$ and $2p_6$ states of neon in Fig. 10. A compilation of these results for both the neon and the sodium lines studied are given in Table III.

E. Consequences of hypotheses

1. Analysis of oscillations from Ne(3p) states*

The experimentally derived cross-section curves were analyzed to obtain the magnitude of the perpendicular ($\perp$) and parallel ($\|$) polarization components of radiation from the oscillatory part of the signal. Figure 11 shows four examples of data analyzed in this manner. These results, expressed as the intensity of the oscillation amplitude (ΔI) at 2-keV beam energy and weighted by the proper branching ratios of Table I, are given in Table IV, column 3.

Each of the 36 molecular state designations [$^1\Sigma^+(0000)$, $^3\Pi(1111)$, etc., where the indices are L, S, Λ, and Σ] was analyzed to determine the mixing coefficients of the asymptotic atomic states, as dictated by hypothesis (c). Molecular states were first transformed into LS coupling-scheme components using standard angular mo-

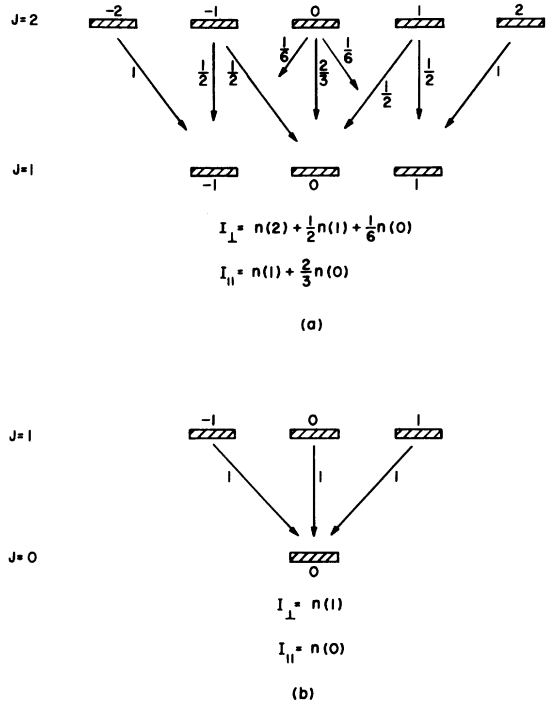

FIG. 10. Transition probabilities (normalized branching ratios) for (a) the $1s_3$-$2p_5$ transition in Ne I, (b) the $1s_5$-$2p_6$ transition in Ne I.

TABLE III. Theoretically derived intensities of the perpendicular and parallel components of radiation from ten lines arising from $2s$-$3p$ transitions in Ne I and two lines arising from $2s$-$3p$ transitions in Na I, expressed in terms of the fractional contributions of each of the M_J upper-state levels, $n(M_J)$. These expressions were obtained in the standard way from rules found in Condon and Shortley (Ref. 16).

State	Line (Å)	Intensity
$^2P_1$	5852	$I_\perp = \frac{1}{3}n(0)$
	$J(1\text{-}0)$	$I_\| = \frac{1}{3}n(0)$
$^2P_2$	6030	$I_\perp = \frac{1}{2}n(1) + \frac{1}{2}n(0)$
	$J(1\text{-}1)$	$I_\| = n(1)$
$^2P_3$	6075	$I_\perp = \frac{1}{3}n(0)$
	$J(1\text{-}0)$	$I_\| = \frac{1}{3}n(0)$
$^2P_4$	6096	$I_\perp = n(2) + \frac{1}{2}n(1) + \frac{1}{6}n(0)$
	$J(1\text{-}2)$	$I_\| = n(1) + \frac{2}{3}n(0)$
$^2P_5$	6266	$I_\perp = n(1)$
	$J(0\text{-}1)$	$I_\| = n(0)$
$^2P_6$	6143	$I_\perp = \frac{1}{3}n(2) + \frac{5}{6}n(1) + \frac{1}{2}n(0)$
	$J(2\text{-}2)$	$I_\| = \frac{4}{3}n(2) + \frac{1}{3}n(1)$
$^2P_7$	6383	$I_\perp = \frac{1}{2}n(1) + \frac{1}{2}n(0)$
	$J(1\text{-}1)$	$I_\| = n(1)$
$^2P_8$	6507	$I_\perp = n(2) + \frac{1}{2}n(1) + \frac{1}{6}n(0)$
	$J(1\text{-}2)$	$I_\| = n(1) + \frac{2}{3}n(0)$
$^2P_9$	6402	$I_\perp = n(2) + \frac{2}{3}n(2) + \frac{7}{15}n(1) + \frac{1}{5}n(0)$
	$J(2\text{-}3)$	$I_\| = \frac{2}{3}n(2) + \frac{16}{15}n(1) + \frac{3}{5}n(0)$
$^2P_{10}$	7032	$I_\perp = \frac{7}{10}n(1) + \frac{3}{10}n(0)$
	$J(2\text{-}1)$	$I_\| = \frac{3}{5}n(1) + \frac{2}{5}n(0)$
Na D_1	5896	$I_\perp = \frac{2}{3}n(\frac{1}{2})$
	$J(\frac{1}{2}\text{-}\frac{1}{2})$	$I_\| = \frac{2}{3}n(\frac{1}{2})$
Na D_2	5890	$I_\perp = n(\frac{3}{2}) + \frac{1}{3}n(\frac{1}{2})$
	$J(\frac{1}{2}\text{-}\frac{3}{2})$	$I_\| = \frac{4}{3}n(\frac{1}{2})$

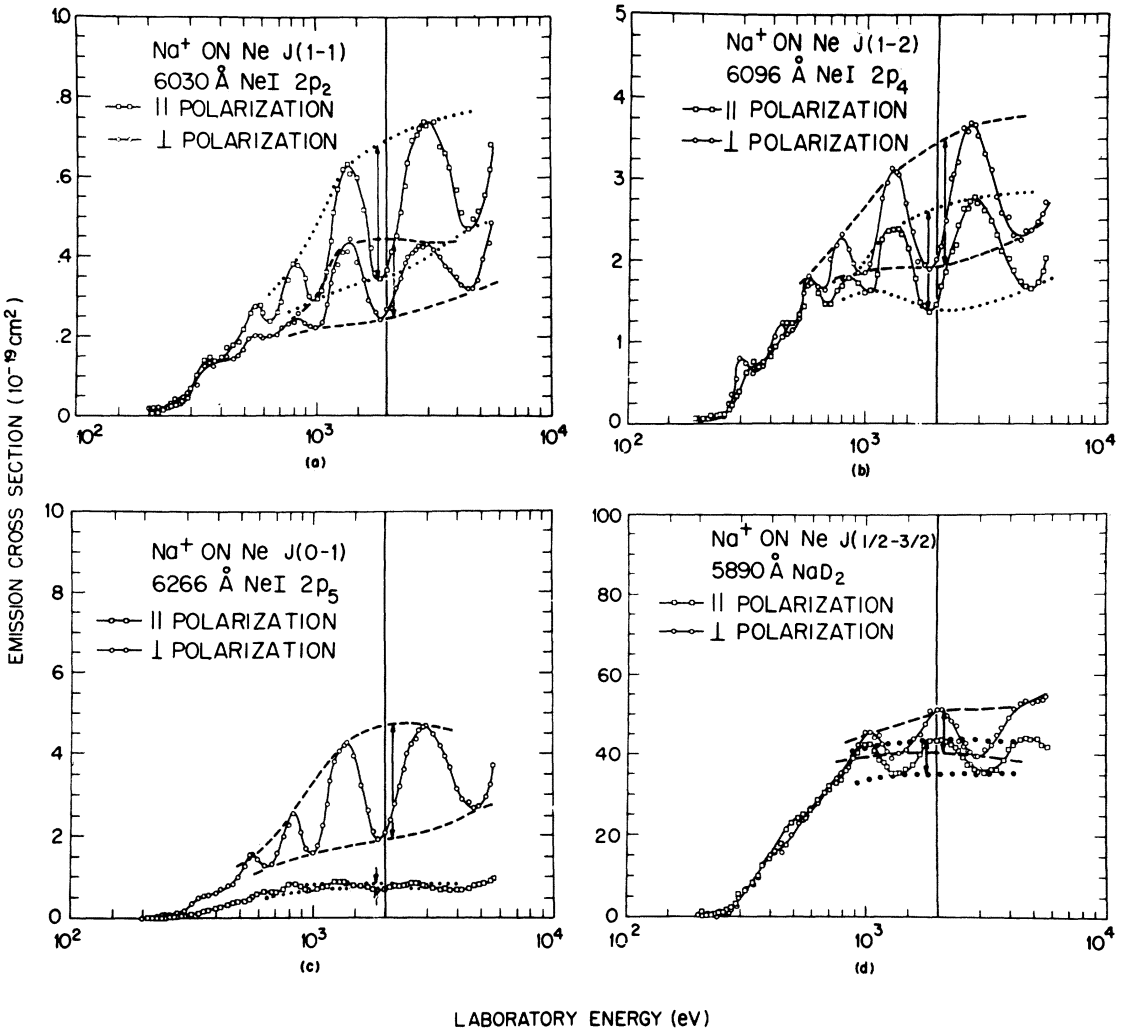

FIG. 11. Absolute emission cross sections for the (a) Ne($2p_2$) 6030-Å, (b) Ne($2p_4$) 6096-Å, (c) Ne($2p_5$) 6266-Å, and (d) NaD_2 5890-Å lines showing the intensity amplitudes ΔI of the regular oscillatory structure for each polarization component as a function of laboratory energy. The vertical arrows show the intensity amplitudes at 2 keV.

mentum coupling techniques.[16] A matrix showing the coupling amplitudes is shown in Fig. 12. Except for $2p_9$ and possibly $2p_1$ and $2p_{10}$, the $2p$ atomic states of Ne I may not be described as pure LS coupling states. Schectman *et al.* have expanded the wave functions of the $2p$ levels in terms of LS functions.[5] These are shown in Table V. Using these intermediate coupling-scheme results we have developed a matrix which relates the $2p$ M_j states to the molecular states. This is shown in Fig. 13 in terms of probabilities. For example, the $^1\Sigma^+(0000)$ state upon dissociation is predicted to produce $2p_1(00)$ with 0.98 probability and $2p_3(00)$ with 0.03 probability, according to hypothesis (c).

By examination of Fig. 13, the striking polarization observed in the $2p_5$ case must be due predominantly to the $^1\Pi(1010)$ state. Only three other molecular states could result in the same polarization, and each of these would put far too much intensity into other transitions to be consistent with experiment. Our first attempt, therefore, was to try to explain the oscillatory structure from all of the Ne* states in terms of a single pair of molecular states of symmetry $^1\Pi(\Omega = \pm 1)$. Note that since L is not a good quantum number at finite internuclear separations, both pairs of $^1\Pi$ states listed in Fig. 13 possess this symmetry. We are therefore free to choose whatever relative

TABLE IV. Experimentally and theoretically derived oscillation amplitude intensities ΔI.

Atomic state [a]	Expt. ΔI at 2 keV (10^{-19} cm^2)	Expt. ΔI adjusted [b]	Theory ΔI $^1\Pi(\Omega=\pm1)$	Theory ΔI $^1\Pi(\Omega=\pm1)+{}^3\Pi(\Omega=\pm2)$
(1)	(2)	(3)	(4)	(5)
$^2P_1$ $\perp$	0	0	0	0
$\parallel$	0	0	0	0
$^2P_2$ $\perp$	0.185	2.05	2.21	2.21
$\parallel$	0.370	4.10	4.42	4.42
$^2P_3$ $\perp$	0	0	0	0
$\parallel$	0	0	0	0
$^2P_4$ $\perp$	1.50	5.02	1.95	4.98
$\parallel$	1.25	4.19	3.90	3.90
$^2P_5$ $\perp$	2.80	6.22	6.50	6.50
$\parallel$	<0.15	<0.33	0	0
$^2P_6$ $\perp$	2.95	6.49	5.63	6.47
$\parallel$	2.70	5.94	2.25	5.61
$^2P_7$ $\perp$	0.80	1.33	0.98	0.98
$\parallel$	1.35	2.24	1.95	1.95
$^2P_8$ $\perp$	1.20	2.10	1.17	1.60
$\parallel$	1.05	1.84	2.34	2.52
$^2P_9$ $\perp$	0.40	0.40	0	0.54
$\parallel$	0.40	0.40	0	0.54
$^2P_{10}$ $\perp$	0.10	0.17	0.09	0.09
$\parallel$	0.10	0.17	0.08	0.08

[a] Expressed in Paschen notation [C. E. Moore, *Atomic Energy Levels*, NBS Circular No. 467 (1949), Vol. 1, p. 76].

[b] Experimental values have been adjusted using branching ratios to reflect population cross-section rather than emission cross-section values.

mixing of these two pairs of states will produce the best possible agreement with experiment. The optimal choice of this mixing, ~1:1, results in the predictions of column 4 of Table IV. Agreement is not satisfactory, particularly for the $2p_4$ and $2p_6$ states.

In order to improve agreement with experiment, it is necessary to include at least one state of symmetry different from $^1\Pi$. We can achieve dramatic improvement by including contributions from the $^3\Pi(\Omega=\pm2)$ states. Column 6 of Table V gives the final predictions, assuming contributions in the following proportions: $^1\Pi(10\pm10):{}^1\Pi(20\pm10):{}^3\Pi(11\pm11):{}^3\Pi(21\pm11)=13:13:6:1.2$. Except possibly for $2p_8$, agreement is excellent.

By inclusion of minor amounts of additional states, slight further agreement could be achieved. But if either the $^1\Pi(\Omega=\pm1)$ or $^3\Pi(\Omega=\pm2)$ states are omitted, agreement cannot be made satisfactory, regardless of how many other states are included to try to compensate.

We conclude from this analysis of the Ne*($3p$) emission that the oscillatory structure in the cross sections can be attributed primarily to a pair of interaction $^1\Pi(\Omega=\pm1)$ states. At least one additional pair of states, $^3\Pi(\Omega=\pm2)$, produces similar oscillations. As shown schematically in Fig. 14, we view these as completely independent paths. Note that oscillations in the $2p_4$ and $2p_6$ states, those to which $^3\Pi(\Omega=\pm2)$ makes its largest contribution, do not quite line up with those in $2p_5$.

2. *Analysis of oscillations from Na*(3p) states*

The $^1\Pi$ and $^3\Pi$(NaNe)$^+$ states can be constructed either from a $^2\Pi$ core and $^2\sigma$ outer electron or from a $^2\Sigma^+$ core and $^2\pi$ outer electron, case (b) or (c) of Table II. We can distinguish between these possibilities by examining the polarization of the Na*($3p^2P_{3/2}$-$3s^2S_{1/2}$) emission. We assume that the symmetry of the Na* excited state is determined solely by the outer electron; the distant

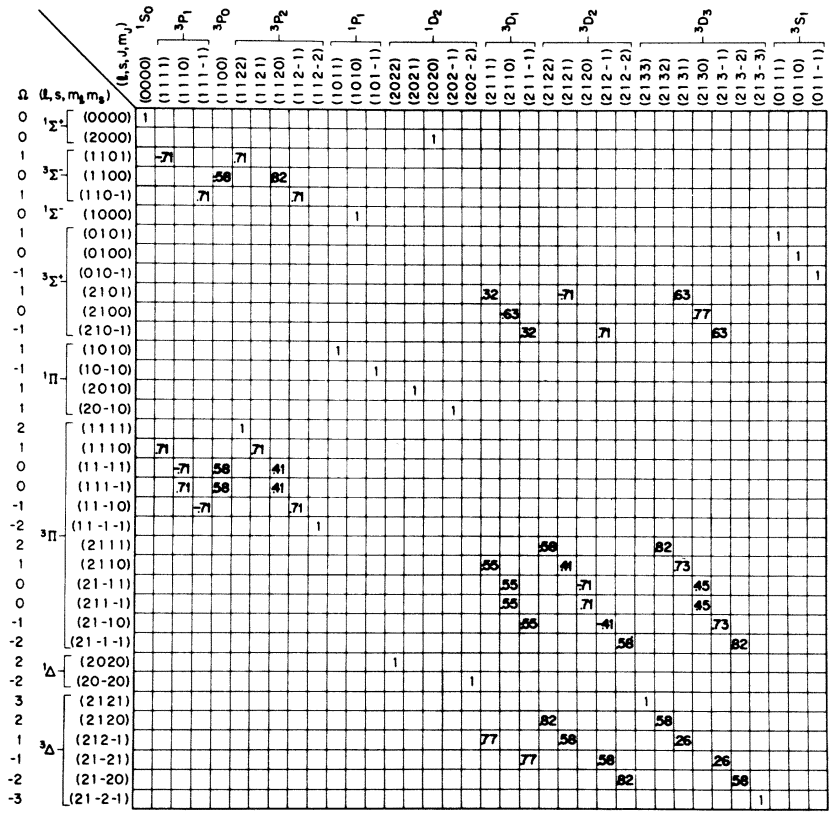

FIG. 12. Transformation matrix written in terms of Clebsch-Gordan amplitudes relating the 36 molecular states ($L S \Lambda \Sigma$) to atomic states ($L S \Lambda \Sigma$) in pure $L S$ coupling.

Ne^+ has no effect. The analysis then parallels that of the Ne* radiation. Invoking part (ii) of hypothesis (c), and making use of the expressions of Table III and standard LS-coupling transformation rules,[16] we obtain the following values for $I_{\parallel}/I_{\perp}$:

$$I_{\parallel}/I_{\perp} = 1.47 \quad \text{for } \sigma \text{ outer electron},$$
$$I_{\parallel}/I_{\perp} = 0.81 \quad \text{for } \pi \text{ outer electron}. \tag{10}$$

In computing these values it was necessary to take account of the effect of hyperfine structure arising from the nonzero spin of the Na nucleus. This, again, was accomplished using standard angular momentum coupling techniques.

The experimentally observed polarization ratio $I_{\parallel}/I_{\perp}$ from the Na($2p_{3/2}$) state is 1.00 ± 0.05. There are three possible explanations for this discrepancy: (i) Hypothesis 3b is incorrect. (ii) Neither of the molecular orbital diabatic schemes, cases (b) and (c) of Table II, are present in pure form. (iii) The $^1\Pi(\Omega = \pm 1)$ states are diabatic states of case (c) of Table II, Σ^+ core and π outer electron, and the $^3\Pi(\Omega = \pm 2)$ states are case (b), Π core and σ outer electron. If this were the case, then the predicted ratio $I_{\parallel}/I_{\perp}$ would be 0.93, in closer agreement with the experimental value of 1.00.

Possibility (i) above is extremely unlikely. Our success in describing the Ne* results is a strong indication that part (i) of hypothesis (c), at least, is valid. As shown in Fig. 1, the Na* levels are much more closely spaced than most Ne* levels; thus the sudden approximation should be more valid for Na* than Ne*, i.e., part (ii) of hypothesis (c) is almost certainly accurate.

Possibility (iii) above predicts a result that is outside our estimated experimental uncertainty, although not by very much. Therefore it appears that possibility (ii) is correct, perhaps in combination with possibility (iii). In conclusion, our results suggest strongly that the simple one-electron diabatic models employed previously[2,3] cannot account adequately for the experimental observations.

3. *Analysis of nonoscillatory emission*

Hypotheses (a)–(d) can be used to analyze the nonoscillatory part of the emission cross sec-

TABLE V. Wave functions for the $2p$ (Paschen notation) levels of Ne I expanded in terms of LS basis functions, taken from the work of Schectman *et al.* (Ref. 5).

States	Intermediate coupling coefficients	States	Intermediate coupling coefficients
$2p_1$ $^1S_0$	0.99	$2p_6$ $^3P_2$	−0.65
$^3P_0$	0.17	$^1D_2$	−0.72
$2p_2$ $^3P_1$	0.80	$^3D_2$	−0.24
$^1P_1$	0.58	$2p_7$ $^3P_1$	0.28
$^3D_1$	−0.02	$^1P_1$	−0.39
$^3S_1$	−0.13	$^3D_1$	0.88
$2p_3$ $^1S_0$	0.17	$^3S_1$	−0.01
$^3P_0$	−0.99	$2p_8$ $^3P_2$	0.13
$2p_4$ $^3P_2$	0.73	$^1D_2$	−0.43
$^1D_2$	−0.55	$^3D_2$	0.89
$^3D_2$	−0.39	$2p_9$ $^3D_3$	1.00
$2p_5$ $^3P_1$	−0.49	$2p_{10}$ $^3P_1$	0.13
$^1P_1$	0.71	$^1P_1$	0.08
$^3D_1$	0.49	$^3D_1$	0.00
$^3S_1$	−0.01	$^3S_1$	0.99

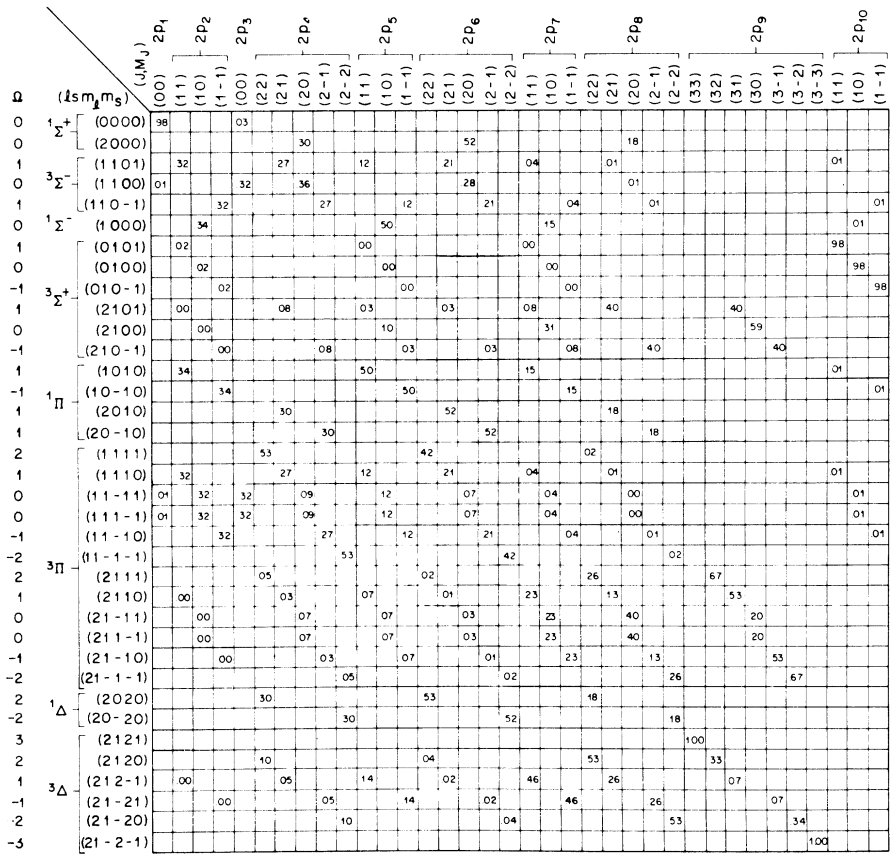

FIG. 13. Transformation matrix written in terms of probabilities (obtained by squaring the amplitudes) relating the 36 molecular states ($L S \Lambda \Sigma$) to the Ne*($3p$) states (JM_j) expressed in Paschen notation. This matrix was derived by taking the product of the matrices in Fig. 12 and Table V.

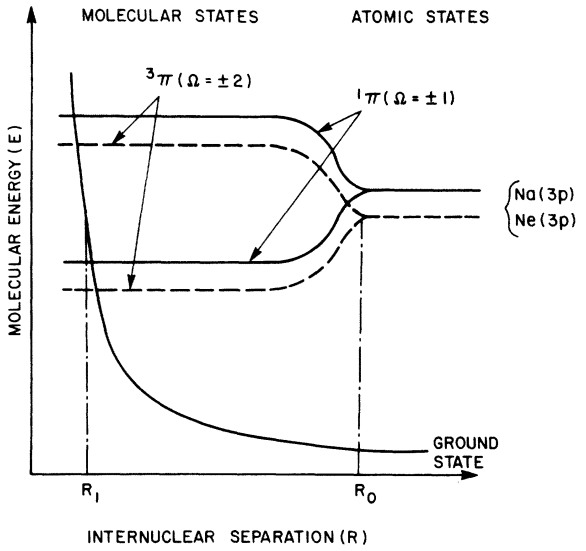

FIG. 14. Schematic illustration of two pairs of coherently excited levels which contribute to the observed quantum-mechanical phase interference.

tions. In the present case it is apparent that a great many molecular states contribute to the incoherent radiation. The complexity of the situation precludes our making a quantitative assessment of the contribution from each state. Nevertheless, we can obtain some important additional information by examination of the nonoscillatory emission.[17]

Our analysis of the Ne* oscillatory emission provides clear evidence that triplet states (specifically, $^3\Pi$) are populated during the collision of Na^+ with Ne. Examination of the nonoscillatory Ne* emission strengthens this conclusion. In particular, radiation from the $2p_{10}$ level must arise predominantly from a $^3\Sigma^+$ molecular state.

The very small cross section for emission of parallel polarized radiation from the $2p_5$ Ne* level is conclusive evidence that the $^1\Sigma^-$ state plays little or no role in the collision process. In fact, the populations and polarizations of all ten Ne*(3p) levels can be accounted for accurately without any contributions from $^1\Sigma^-$, $^3\Sigma^-$, $^1\Delta$, or $^3\Delta$ states. This does not rule out the possibility that some of these states participate, but we can say at least that both oscillatory and nonoscillatory results appear consistent with dipole selection rules,

$$\Sigma^+ \rightarrow \Sigma^+, \Pi,$$

$$\Sigma^+ \not\rightarrow \Sigma^-, \Delta.$$

The fact that triplet states are populated is perhaps not very surprising. The initial excitation process is a direct excitation of the Ne atom; i.e., it does not involve charge transfer or Na^+ excitation. This is apparent from the fact that the phase shift $\Delta\varphi_0$ of Eq. (8) is an integral multiple of 2π for the Ne* emission. The 3p levels of the isolated Ne* atom are known to be significantly mixed by spin-orbit coupling[4,5]; thus it is certainly possible that the corresponding levels in the $(NaNe)^+$ are also mixed. On the other hand, the $(NaNe)^+$ molecular states appear to be pure spin states at intermediate internuclear separations. This is true at least for the $^1\Pi(\Omega=\pm1)$ state that is primarily responsible for the oscillations. The contribution of $^3\Pi(\Omega=\pm1)$ states to the oscillations can be demonstrated to be negligible. Note that nowhere in the present analysis has it been assumed that the molecular states can be characterized by definite values of spin and/or orbital angular momentum. Rather, the fact that Σ and Λ appear to be good quantum numbers in the intermediate separation region, at least for the $^1\Pi(\Omega=\pm1)$ state, follows directly from the experimental results and hypotheses (a)-(d).

V. CONCLUSIONS

Using plausible hypotheses we have been able to account quantitatively for the amplitudes and polarizations of the oscillatory structure in the emission cross sections of 3p levels excited in collisions of Na^+ with Ne. Our analysis of the data provides evidence that the oscillatory behavior arises predominantly from two independent pairs of molecular states, $^1\Pi(\Omega=\pm1)$ and $^3\Pi(\Omega=\pm2)$, as illustrated schematically in Fig. 14. These states are populated coherently at small internuclear separations, evolve independently as the collision partners recede, and finally interact via a charge transfer mechanism at large (~10–15 Å) internuclear separations. Extension of the analysis to the nonoscillatory results provides further evidence that both singlet and triplet states are produced in the initial excitation process, and suggests that only Σ^+ and Π states play a major role in the excitation.

The validity of the model presented here is supported by its simplicity and by its success in accounting quantitatively for the very detailed and complicated experimental results. The model is a very general one which we believe will be valuable in elucidating the mechanisms of many low-energy ion-atom collision processes.

ACKNOWLEDGMENT

The authors are grateful to V. Kempter for helpful discussions.

*Research supported in part by NSF Grant No. GF43976.

[1](a) N. H. Tolk, C. W. White, S. H. Dworetsky, and L. A. Farrow, Phys. Rev. Lett. 25, 1251 (1970); S. Dworetsky, R. Novick, W. W. Smith, and N. Tolk, *ibid.* 18, 939 (1967); R. F. Stebbings, R. A. Young, C. L. Oxley, and H. Ehrhardt, Phys. Rev. 138, A1312 (1965); M. Lipeles, R. Novick, and N. Tolk, Phys. Rev. Lett. 15, 815 (1965); (b) V. A. Ankudinov, S. V. Bobashev, and V. I. Perel, in *Proceedings of the Seventh International Conference on the Physics of Electronic and Atomic Collisions,* edited by T. R. Govers and F. J. de Heer (North-Holland, Amsterdam, 1971), p. 581.

[2]N. H. Tolk, C. W. White, S. H. Neff, and W. Lichten, Phys. Rev. Lett. 31, 671 (1973).

[3]T. Andersen, A. Nielsen, and K. J. Olsen, Phys. Rev. Lett. 31, 739 (1973).

[4]W. R. Bennett and P. J. Kindlmann, Phys. Rev. 149, 38 (1966).

[5]R. M. Schectman, D. R. Shoffstall, D. G. Ellis, and D. A. Chojnacki, J. Opt. Soc. Am. 56, 1585 (1966).

[6]S. V. Bobashev, Zh. Eksp. Teor. Fiz. Pis'ma Red. 11, 389 (1970) [JETP Lett. 11, 260 (1970)]; Ref. 1(b), p. 32. Oscillatory structure observed by Bobashev in the collisional excitation of the Ne I resonance lines by Na^+ appear to have the same spacing and approximate phase as we have observed in the Na *D* levels. However, Bobashev's measurements do not have the same spacing as the charge exchange oscillations measured by Z. Z. Latypov and A. A. Shoporenko even though the levels are near degenerate at large internuclear distances.

[7]Z. Z. Latypov and A. A. Shoporenko, Zh. Eksp. Teor. Fiz. Pis'ma Red. 12, 177 (1970) [JETP Lett. 12, 123 (1970)].

[8]V. A. Ankudinov, S. V. Bobashev, and V. I. Perel', Zh. Eksp. Teor. Fiz. 60, 906 (1971) [Sov. Phys.—JETP 33, 490 (1971)].

[9]N. H. Tolk, C. W. White, S. H. Dworetsky, and D. L. Simms, in *Proceedings of the Seventh International Conference on the Physics of Electronic and Atomic Collisions, Amsterdam, 1971,* Abstracts of Papers, edited by L. M. Branscomb *et al.* (North-Holland, Amsterdam, 1971), p. 584.

[10]A preliminary account of this model was reported by N. Tolk, J. C. Tully, C. W. White, J. Kraus, A. A. Monge, and S. H. Neff, Phys. Rev. Lett. 35, 1175 (1975).

[11]H. Rosenthal and H. M. Foley, Phys. Rev. Lett. 23, 1480 (1969); H. Rosenthal, Phys. Rev. A 4, 1030 (1971).

[12]W. Lichten, Phys. Rev. 139, A27 (1965).

[13]Excitation of inner-shell electrons [such as Na(2*p*) or Ne(2*s*)] appears to be possible on the basis of united-atom–limit considerations. Such an excitation would produce autoionizing states which would not lead to any of the lines observed in the present study. We therefore ignore such transitions.

[14]G. Herzberg, *Molecular Spectra and Molecular Structure I. Spectra of Diatomic Molecules* (Van Nostrand, Princeton, N. J., 1950), 2nd ed., p. 318.

[15]See, for example, Fig. 3 of Ref. 2.

[16]E. U. Condon and G. H. Shortley, *The Theory of Atomic Spectra* (Cambridge U. P. New York, 1959, pp. 45–78.

[17]An attempt to do this at higher collision energies using assumptions related to ours has been reported by E. E. Nikitin, M. Ya. Ovchinnikova, and A. I. Shushin, Zh. Eksp. Teor. Fiz. Pis'ma Red. 21, 633 (1974) [JETP Lett. 21, 299 (1975)].